Solid Freeform Fabrication 2025: Proceedings of the 36th Annual International Solid Freeform Fabrication Symposium – An Additive Manufacturing Conference
Reviewed Paper

Design, Additive Manufacturing, and Compression Response of a Novel Triply Periodic Interlaced Surface (TPIS) Meta-Material

A. Prey*, N. Giusti*, Z. Okun*, Y. Mistry*, and D. Bhate*

*3DX Research Group, School of Manufacturing Systems and Networks, Ira A. Fulton Schools of Engineering, Arizona State University, Mesa, AZ 85212

Abstract

Prior to the advances in Additive Manufacturing (AM), cellular materials were primarily either honeycombs or foams, with their design possibilities constrained by manufacturability. However, in the last two decades, AM has enabled beam-based lattices, surface-based TPMS structures and a wide range of novel design ideas for meta-materials such as interpenetrating and interwoven lattices. In this work, we propose a new class of meta-materials derived from a form we term Triply Periodic Interlaced Surface (TPIS), which are inspired by TPMS geometries in their functional origins but are interlaced in a manner similar to basket weaving. We demonstrate the parametric design of these meta-materials and use Selective Laser Sintering (SLS) to fabricate them, followed by testing under compression. Results show that the TPIS structures hold promise for their ability to achieve high compliance at high relative densities, with the potential for application in energy absorption, piezoelectric sensing and energy harvesting.

Keywords

Additive manufacturing, TPIS, cellular material, compression testing, design

Introduction

Inspiration for the design of cellular (also called architected, or meta-) materials has come from many sources. Arguably the first engineered cellular materials were honeycombs and foams [1], both of which were inspired by biological forms and enabled by the manufacturing processes available in a world before Additive Manufacturing (AM) came along. With the advent of AM, bio-inspired design of these materials has only accelerated [2], [3]. Another source of inspiration comes from the beam based, lattice-like trusses in civil engineering that were leveraged in the construction of bridges and led to Maxwell's stability criterion [4], a concept invoked in the study of much smaller lattice materials today [5]. Crystallography has also been leveraged to develop lattice shapes that share names with metallic crystal structure such as BCC (Body Centered Cubic) and FCC (Face Centered Cubic) [3]. Mathematics has also been leveraged to derive cellular material geometry, most emphatically in the design of Triply Periodic Minimal Surface (TPMS) based materials [6], [7], [8]. More recently, computational approaches such as simulation driven topology optimization [9], [10] and generative Artificial Intelligence (AI) methods have been applied to the problem of cellular material design [11], [12], [13]. This work differs from the above in seeking its inspiration for design from traditional handicrafts, particularly the so-called "plaited crafts", and primarily basket weaving.

Baskets and woven mats are among the oldest plant-based crafts found around the world [14], and incorporates a wide range of insight and considerations developed over centuries. Baskets can be woven with a wide range of materials, and as shown in Figure 1, different types of weaves. Each of these weave patterns possesses a certain functional benefit and conveys aesthetic meaning, while also embodying underlying skill in their creation, often passed down across generations. This work limits itself to three aspects of basket weaving and associated research questions with each:

- Design: *How can a primarily two-dimensional concept of weaving to create objects such as baskets be translated into space-filling three-dimensional design?*
- Manufacturing: *How can such 3D woven materials be represented in computational design and manufactured so as to have structural integrity and enable further characterization and testing?*
- Properties: *What properties can we expect to obtain from such woven, 3D materials that may make them attractive candidates for engineering applications?*

Figure 1. Examples of basket weave patterns – why are there few space-filling, 3D architected additively manufactured meta-materials that leverage these woven patterns? This work is inspired by this question and is a preliminary effort to address this question (all images in public domain, no attribution needed)

While this article does not provide comprehensive answers to any of these questions, it makes preliminary incursions into each of these three domains – this is also how the rest of the paper is structured. Before commencing a discussion of the work conducted here, it is however important to review the literature related to the above questions. Several attempts have been made in defining, digitizing and modeling woven materials – be they for forms represented in fabric and textile composites [15], [16], [17], or plaited crafts such as the baskets [18], [19] discussed here. Most of this work has focused around modeling these woven structures for understanding their

construction and behavior, but not necessarily translating it into designs for additive manufacturing. Nonetheless, forms that resemble woven geometries have been designed and additively manufactured, including interpenetrating lattices, which while not strictly woven, resemble these forms by hybridizing two non-intersecting lattices in one form [20]. Other strategies to create similar forms include creating lattices where each strut itself is braided [21], and decoupling traditional lattices such as the BCC lattice at their nodes [22].

This work distinguishes itself from prior efforts by creating truly woven forms that resemble the up-and-down nature of weaves by leveraging simple mathematical functions in a manner similar to those used in the development of TPMS structures. It also borrows the terminology of TPMS – since these forms are not minimal surfaces with zero mean curvature, the M is replaced with an I – for interlaced, resulting in TPIS: Triply Periodic Interlaced Surfaces. In this work, true periodicity is not demonstrated, but the authors believe future and more rigorous mathematical work can demonstrate this to be true, or develop the modifications needed to arrive at this. The next section discusses the design aspects of this work – from the initial mathematical basis to its implementation in form-generating software. This is followed by a discussion of the AM of the specimens used in study. While several tests could be performed on these specimens, this work focuses on quasistatic compression, results of which are then presented. This is followed by a discussion that motivates the potential applications for these materials, followed by a conclusion discussing limitations of this work, and the associated challenges with addressing them.

Design

To develop the basket-inspired TPIS structures at the center of this work, components were created using the Grasshopper plugin in Rhino 7 [23], as shown in Figure 2 for the simple case of generating a sine wave, defined as a function *x*sin(y)*, with points defined at equal intervals. Specifying different values for the variable *x* and *y* allows the generation of different curves. While this work only used this simplest of sinusoidal functions, more complex curves can be explored as well using this method – in a manner similar to the different mathematical functions that underlie TPMS geometries. The selection of the *sin* function for this work was done for convenience only. These curves can then be mapped onto a grid as shown in Figure 3a, and each curve can then be assigned a certain geometry as an extruded cross-section that projects along the curve, as shown for a circular cross-section in Figure 3b. However, these can also be rectangular sections, creating a basket-like weave, as shown in Figure 3c. The weave shown here, to use this work's terminology, is a "1-plane" weave – while technically not a true plane with regard to the solid elements, it expresses the idea that the neutral axes for the sinusoidal curves for all woven elements are contained in a single plane.

While 1-plane structures like those in Figure 3c can be vertically stacked to achieve space filling, this configuration alone does not ensure true 3D weaving with sufficient inter-weave contact, which is critical to maintaining structural integrity and preventing collapse. Figure 4a shows a 2-plane structure that addresses this: the first plane, shown in green, is a stacked structure with the 1-plane weave shown in Figure 3c. To this is added a second plane, shown here going into the plane of the paper, in red color, making a 2-plane structure. Remarkably, it is possible to add a third plane, as shown in Figure 4b. While this is challenging to visualize, labeling each of the two sinusoidal elements that make up a paired woven plane, as shown in Figure 4c, enables identifying the three different planes that make up the 3-plane structure. The rest of this work

involves testing both the 2-plane and 3-plane structures, and they are identified as such going forward. It must be noted however that it is only the 3-plane structures that may be considered truly triply periodic since 90 degree rotations in any direction recover the same geometry, though the mathematical proof of this is beyond the scope of the present work.

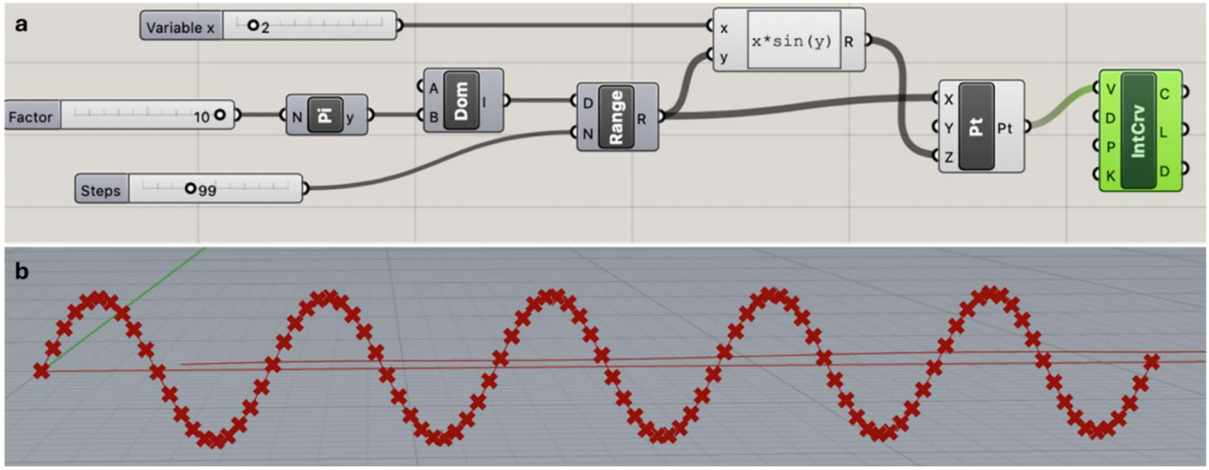

Figure 2. Design activities in this work were executed using (a) components in Grasshopper plug-in in Rhino 7 [24] that can be used to (b) create geometric forms such as a simple sine-wave curve, and extended to 3D shapes in this work

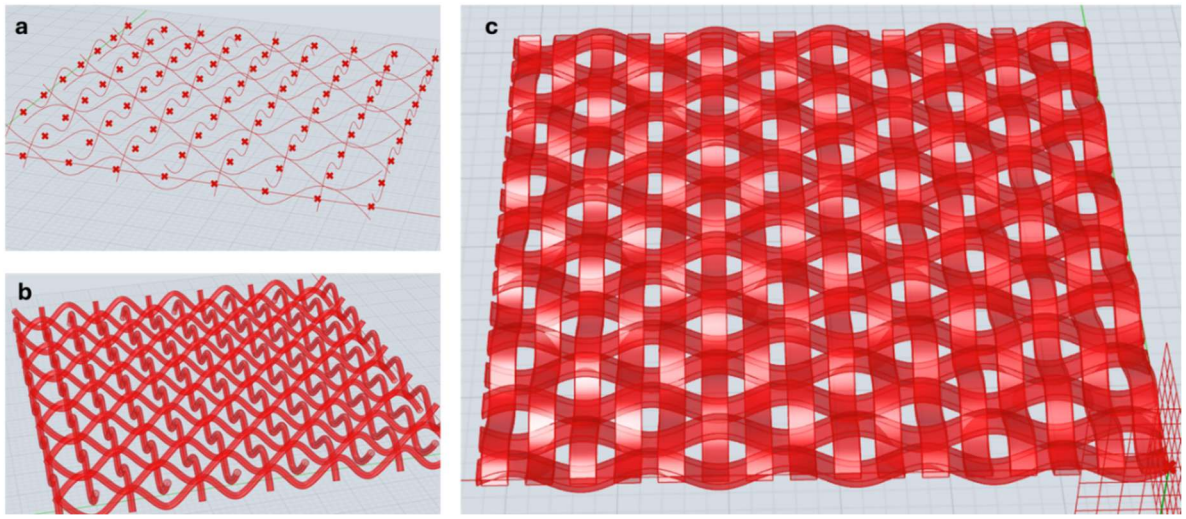

Figure 3. The steps in creating a basket-like matrix for a "1-plane" weave structure: (a) defining a grid of points along sinusoidal curves, (b) connecting these points with solid struts, or (c) flat strips similar to ones found in baskets

To enable mechanical testing under compression, specimens were designed to fill a 50 x 50 x 50 mm envelope, with edges trimmed as needed at the boundary of the envelope. End caps were added at the top and bottom of each structure designed, as shown in Figure 4d – these were 5mm thick and conformed to the outer boundary of the envelope. The Grasshopper script for the full 3D geometry of a 3-plane TPIS structure with end caps for compression testing is available in the link provided as supplementary material at the end of this article. For this study, a total of 12 specimens were designed for additive manufacturing using the Selective Laser Sintering (SLS) process. Three different design inputs were part of the experimental evaluation: (i) the number of

planes, as discussed above: 2-plane and 3-plane; (ii) the unit cell size, which directly informs the number of cells in the specimen in each direction: 4x4x4, 5x5x5 and 6x6x6; and lastly, (iii) the cross-sectional dimensions of the members: in principle, each member had a rectangular section (though this is not required) – to keep variables limited, a square section was selected for this study, with variable thicknesses that were chosen by examining the design to ensure there was sufficient clearance. For smaller cells, for example, it is essential that the thickness is not excessively large, to ensure the elements do not merge. On the other hand, making the elements too thin relative to the available space would result in a potential loss of the contact benefits between weave elements. Table 1 lists all the twelve design combinations explored in this work – no replications were conducted in this study. Opportunities for improvements in the design of this experiment are discussed in the penultimate section.

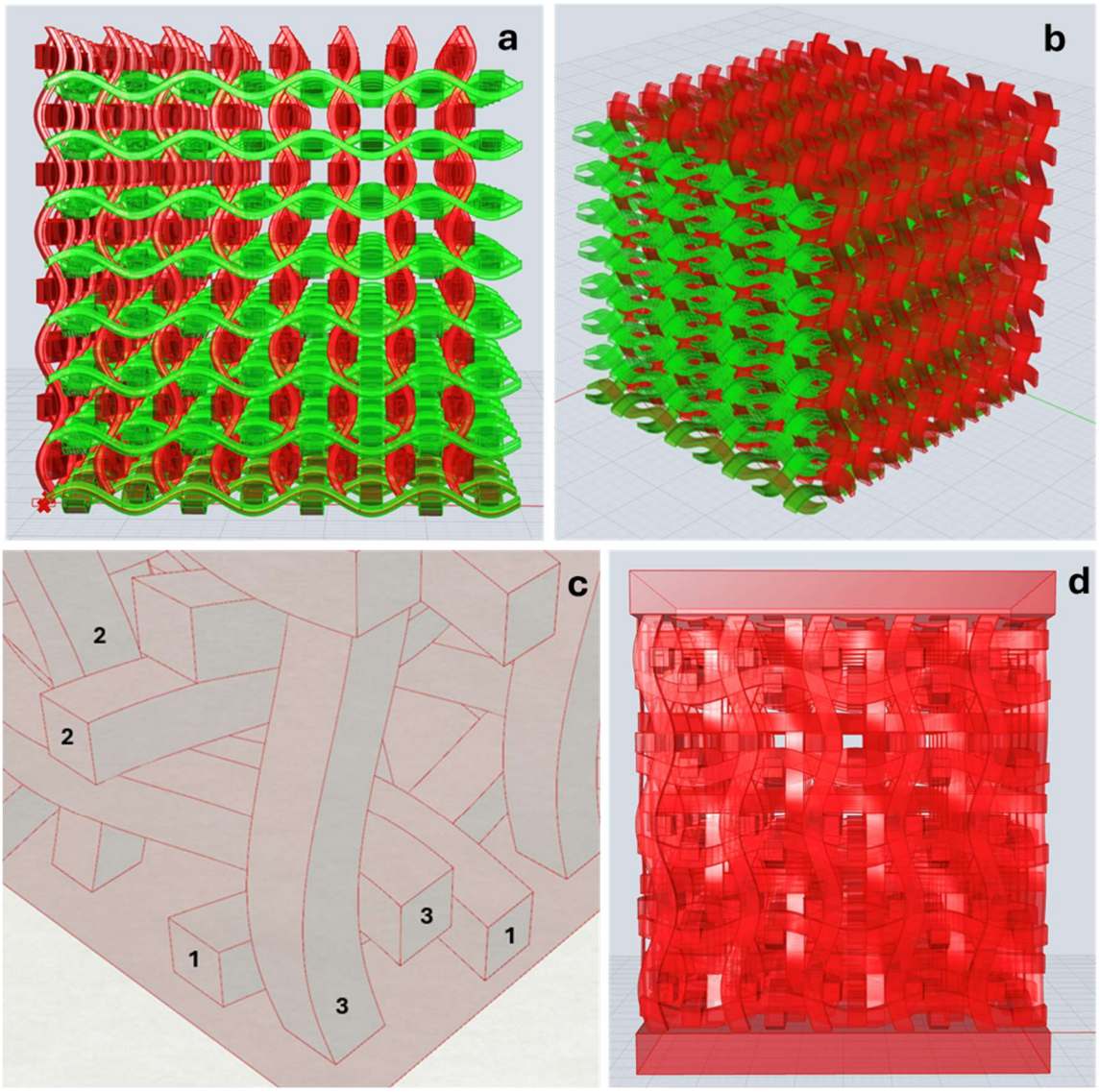

Figure 4. (a) Front view of a 3D space-filling woven meta-material with only two planes – a horizontal plane and a vertical one, (b) isometric view of a complete 3D Triply Periodic Interlaced Surface (TPIS) structure, showing three interlaced, non-intersecting planes, and (c) design with 5mm caps on top and bottom prior to 3D printing and testing

Table 1. Test plan for exploring the design and mechanical behavior of TPIS meta-materials in this work – a total of 12 specimens were designed for this study

Label	Number of Planes	Unit Cell Layout	Strip Thickness (mm)
2-plane, 4x4x4, 2.50mm	2	4x4x4	2.50
2-plane, 4x4x4, 3.25mm	2	4x4x4	3.25
2-plane, 5x5x5, 2.25mm	2	5x5x5	2.25
2-plane, 5x5x5, 2.75mm	2	5x5x5	2.75
2-plane, 6x6x6, 1.75mm	2	6x6x6	1.75
2-plane, 6x6x6, 2.25mm	2	6x6x6	2.25
3-plane, 4x4x4, 1.75mm	3	4x4x4	1.75
3-plane, 4x4x4, 2.25mm	3	4x4x4	2.25
3-plane, 5x5x5, 1.50mm	3	5x5x5	1.50
3-plane, 5x5x5, 2.00mm	3	5x5x5	2.00
3-plane, 6x6x6, 1.25mm	3	6x6x6	1.25
3-plane, 6x6x6, 1.75mm	3	6x6x6	1.75

Manufacturing

Selective Laser Sintering (SLS) was selected as the process for the manufacturing of the TPIS structures since each element within the structure is by design not making contact with another. This rules out the possibility for self-supporting design, which is common in many TPMS designs. SLS, which is a powder bed process, is able to fabricate most parts without need of supports and as such was used to fabricate these structures, with Nylon-12 (EOS^{TM} PA-2200) as the material [25]. All 12 specimens fit at the bottom of the build envelope, as shown in Figure 5a. The parts were manufactured on an EOS Formiga P110 machine (Figure 5b) and post-processed with bead-blasting (Figure 5c). Each specimen was weighed on a precision analytical balance with a resolution of 0.1 mg.

Figure 6 shows ten of the 12 specimens fabricated using this process that were free of gross defects. Two kinds of gross defects were seen in two of the specimens, and are shown in Figure 7. The underlying cause for both is the very large relative clearance, a result of large cell size and/or thin element thickness. This results in either elements that slide out entirely from the structure, or elements that slide off their intended axis. Another possible defect is the merging of elements into each other, but this was prevented in this build by visual inspection in the Rhino software prior to manufacturing. While data was still collected from all 12 specimens, the two defective specimens are identified in subsequent analysis.

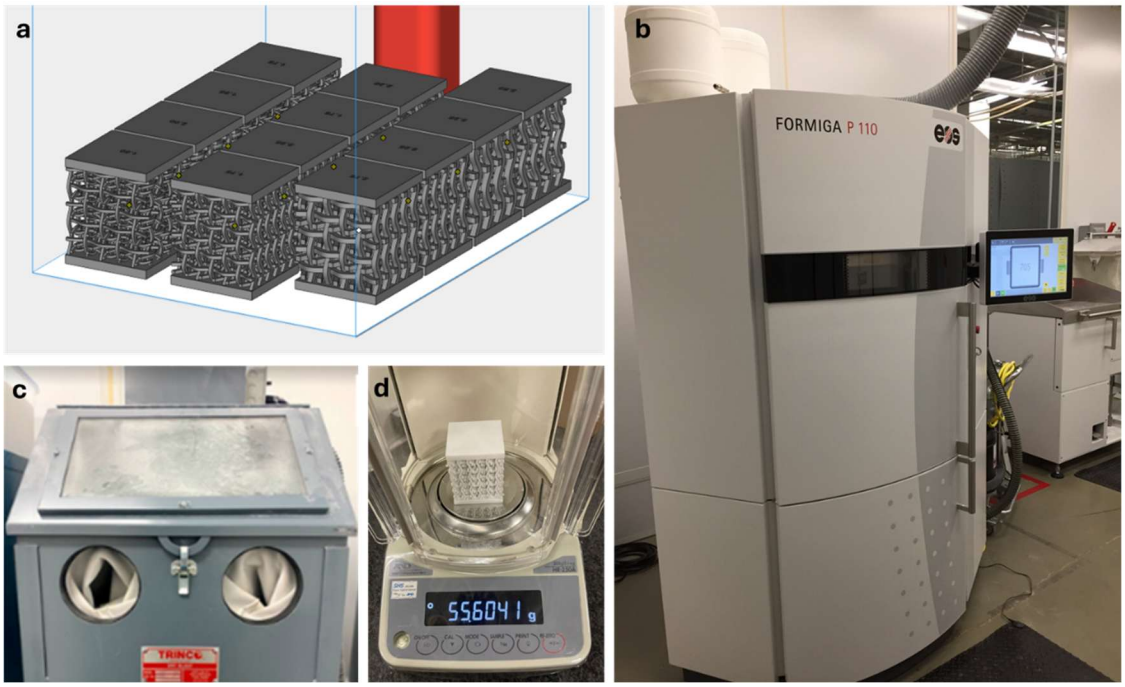

Figure 5. Selective Laser Sintering (SLS) of (a) a total of 12 specimens, showing build layout, setup for the (b) EOS Formiga P110 SLS machine, (c) parts were bead blasted with silica beads after printing, washed and (d) weighed on a precision balance for the estimation of relative density

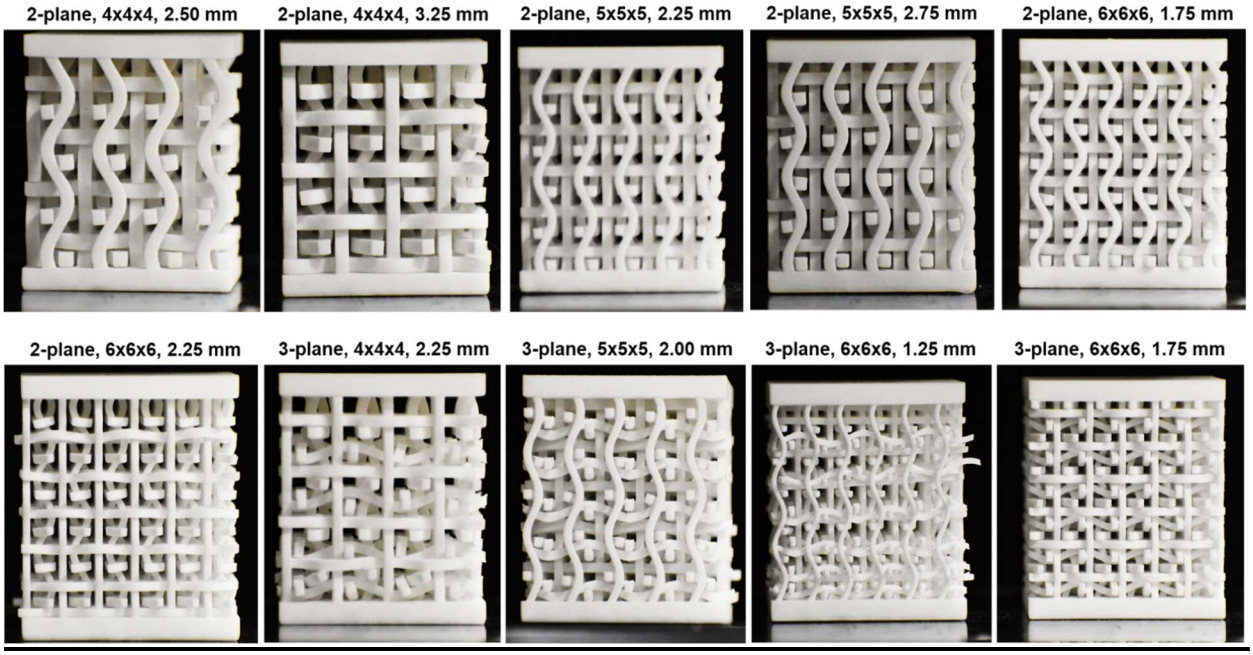

Figure 6. Ten of the twelve SLS printed specimens that were successfully fabricated without gross defects – headers indicate type of design (number of planes, XxYxZ cell layout, thickness of the strips).

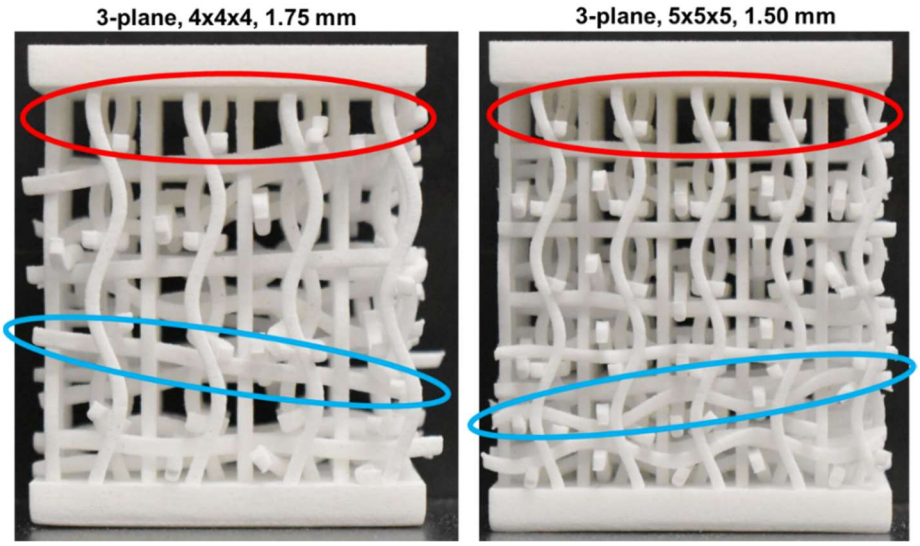

Figure 7. Two specimens (3-plane, 4x4x4, 1.75mm, and 3-plane, 5x5x5, 1.5mm) had defects due to excessively large clearances, manifest as missing elements (top red ellipse) or slanted elements (bottom blue ellipses)

Compression Response

To study the mechanical behavior of the TPIS structures, compression tests were conducted on an Instron 5848 universal testing machine [26], following a setup and procedure developed and described elsewhere, employing a video extensometer for tracking displacement and a digital SLR camera capturing video for analyzing compression patterns [27]. The test was run in displacement control, calculated to result in an effective strain rate of 0.001 s^{-1}. While prior work has suggested this strain rate is not truly quasistatic for polymeric cellular materials [28], it is low enough to exclude dynamic effects and enable meaningful comparisons across designs. Estimated load and displacement are normalized to an effective stress (σ^*) and strain (ε^*) using the build envelope area (50x50 mm^2) for the former, and the height of the specimen, not including the end caps (50 mm) for the latter, following best practices in this regard [29]. A typical effective stress - effective strain curve (σ^*-ε^*) is shown in Figure 8a, for the 2-plane and 3-plane specimens, both with a cell layout of 6x6x6, and with 1.75mm thick elements. Compression data for all other specimens is available in the supplementary materials.

A cursory examination of the two curves plotted show that both specimens have a brief linear region at very low strain rates, associated with the elastic, pre-buckling response of the structure. Following a first peak, the two specimens show different responses. The 3-plane specimen, with its higher relative density, demonstrates a hardening response, while the 2-plane specimen has a flat plateau, even demonstrating slight softening. What is remarkable for both curves is the absence of any undulations in the plateau region. For the 2-plane structure particularly, the large onset strain of densification, coupled with the distinct first peak and low undulations make it a prime candidate for energy absorption applications [30]. Compression patterns taken at five different strain points (including the unstrained state) are shown in Figures 8b and 8c for the two different specimens. The first peak coincides with onset of buckling in the

vertical beams. With further compression, the 3-plane structure forms an hourglass shape but the 2-plane structure deflects to a preferential side due to fewer constraints and breaks symmetry. The additional constraining effect of the third plane is likely the cause of the hardening seen in the 3-lane structure, which is absent in the 2-plane specimen.

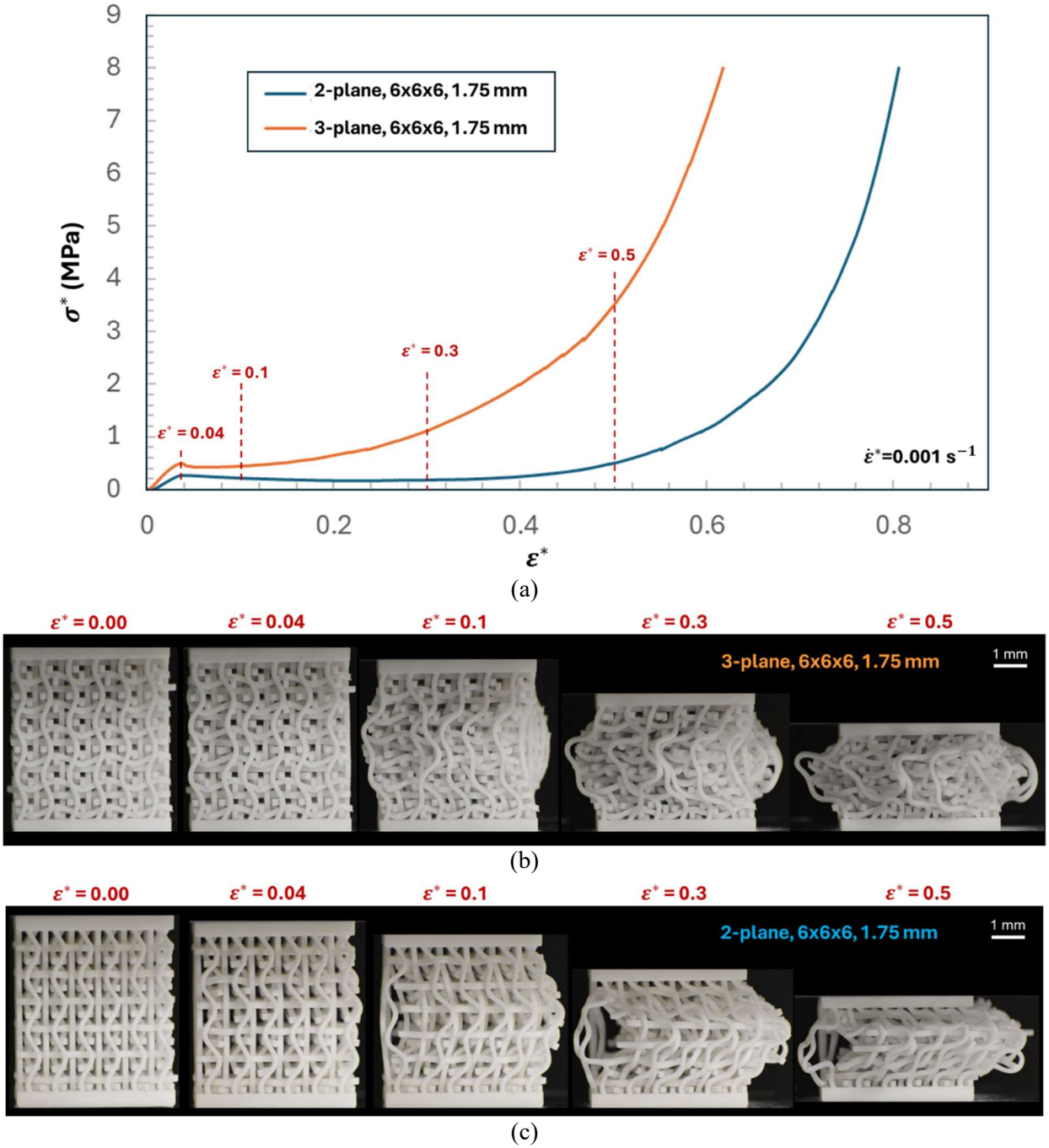

Figure 8. (a) Typical compression response for a TPIS structure, tested at a strain rate of 0.001 s^{-1}, shown here for a 3-plane, 6x6x6 with 1.75mm thick strips. Dotted red lines indicate strain points corresponding to deformation patterns during compression for (b) the 3-6x6x6-1.75mm, and (c) 2-6x6x6-1.75mm specimens

The effective stress-effective strain curves allow for the computation of the effective elastic modulus (E^*) by honing in on the linear region at the start of the curve and performing a linear fit till the regression value exceeds 0.99. This effective modulus can be then normalized by the modulus of the base material (E_s), in this case, Nylon-12, with a reported elastic modulus of 1650 MPa from the supplier datasheet [25]. These values for all 12 specimens are shown in Figure 9a, with the two defective specimen results indicated with orange arrows. The variations in effective modulus are, as is to be expected, primarily from changes in geometry resulting in variations in relative density, as shown in Figure 9b. The 2-plane structures have a slightly higher effective modulus for a given relative density, but this is likely due to the additional density of the 3-plane structures that do not contribute to load transfer along the compression direction.

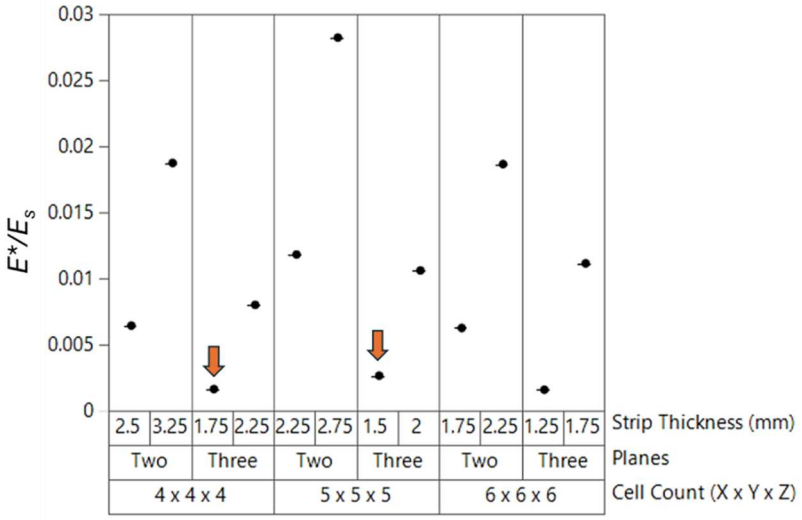

(a)

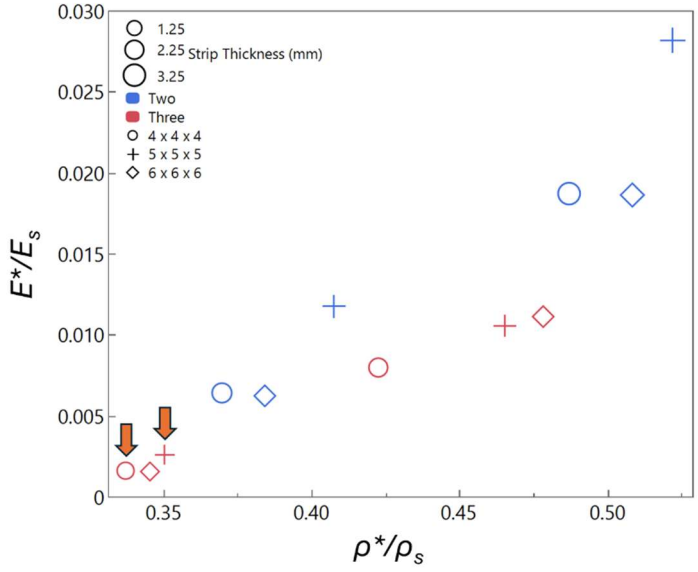

(b)

Figure 9. (a) Normalized effective elastic modulus (E^*/E_s) of the specimens in this study – the two arrows point to the defective specimens with loose strips and are included here for completeness, and (b) E^*/E_s plotted as a function of relative density, with marker size, color and shape indicating thickness, number of planes, and unit cell layout, respectively

Discussion

While this work was designed as a preliminary, empirical study into the design, manufacturability and compression behavior of a new meta-material concept called TPIS, with no attempts to optimize behavior for meeting a particular objective, it is useful to examine the interesting properties of this material and potential applications that leverage them. First of these is the effective modulus discussed previously. A way to interpret the relevance of the results reported here, it is useful to create an Ashby plot and compare the normalized effective modulus (E^*/E_s) against other reported literature. Data from a prior publication [22]was used to generate the Ashby plot shown in Figure 9, with the data obtained in this study superimposed on the graph, shown with the indicated red bubble. These structures are very compliant, with stiffnesses among the lowest reported in the literature for a given relative density. This may be expected given the significant number of elements that at any given time are only loosely connected to the others, and not participating in load transfer. Simulation would be needed to verify if this is truly the case, and to draw more insight on the role of contact, friction and buckling. Nonetheless, this relative low compliance for a given relative density suggests applications in piezoelectric sensing and energy harvesting, where high compliance at high densities can result in greater piezoelectric output per unit applied load.

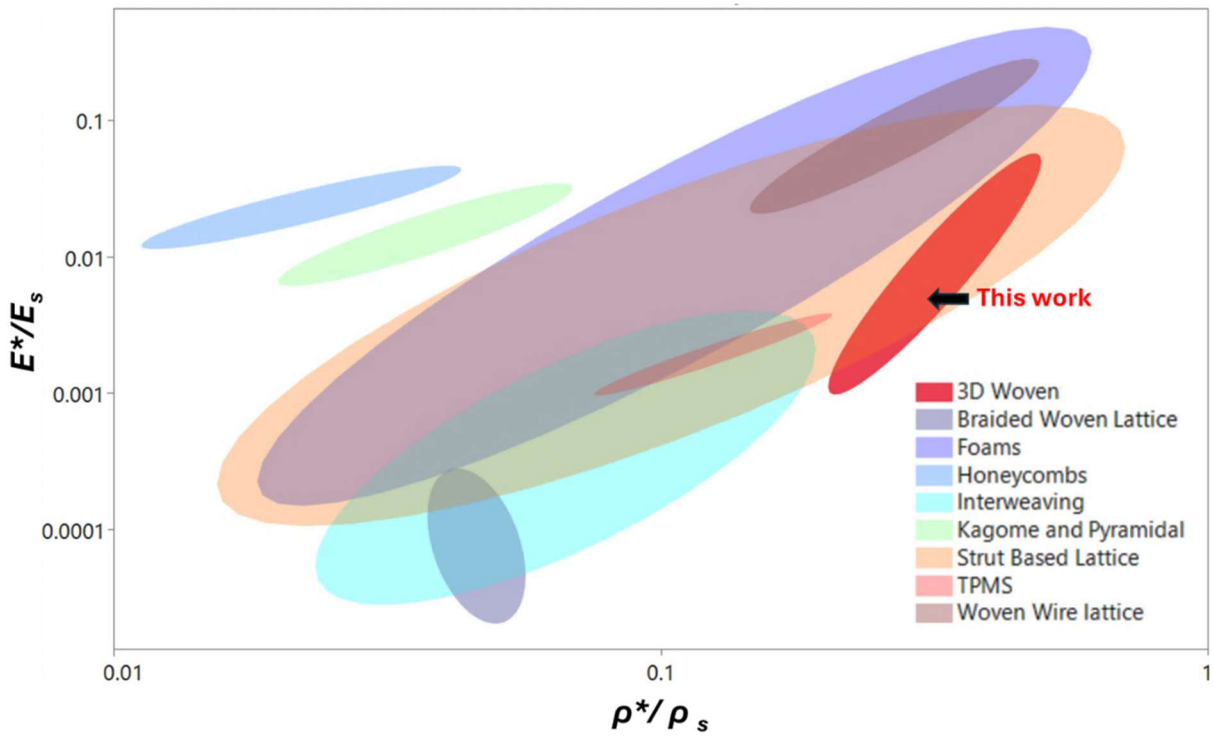

Figure 10. Log-log Ashby plot relating normalized effective modulus *(E^*/E_s)* and relative density (ρ^*/ρ_s), with reference data from prior work [22], with the results obtained from this work shown in the red bubble. The 3D woven meta-materials in this work are among the most compliant (for a given relative density) reported in the literature.

Another key observation, mentioned previously, is that the compression response beyond the first peak that approaches an ideal energy absorber with regard to a distinct first peak and a nearly flat plateau (for the 2-plane structure) with high onset strain of densification. This suggests applications in energy absorption. Further, the dense, network like structure of the TPIS forms may also make them candidates for filtration applications. More work is needed to explore these application possibilities.

Conclusions

This work sought to propose a new meta-material inspired by basket weaving and based on TPMS-like mathematical functions. It showed how such structures may be constructed from simple sinusoidal curves and extended to develop 2- or 3-plane structures. It also showed these structures can be manufactured with the Selective Laser Sintering (SLS) process, and specimens so fabricated showed high compliance and promising energy absorption behavior under compression.

Much work remains to be done, beginning with addressing the limitations of this work. For one, the claimed periodicity in three directions remains to be proven mathematically. Secondly, little is understood about the guidelines around different design parameters to ensure a true woven structure is arrived at, with no intersections between the elements and limited clearance that ensures the structure retains its geometric intent. Nonetheless, it is hoped that this work initiates future work to address these questions, as well as translate these observations to application.

Supplementary Materials

Grasshopper scripts and compression from this work are uploaded and freely available online at the following links - script at: https://data.mendeley.com/datasets/k6zjp7kf9k/1, and compression data at https://data.mendeley.com/datasets/tj6nhc4t6w/1. This includes Grasshopper scripts to generate the basket-inspired TPIS structures discussed here, and compression test raw data for all 12 specimens. Videos of all compression tests are available on request from the corresponding author by email: Dhruv Bhate, dpbhate@asu.edu.

References

[1] L. Gibson and M. Ashby, “Cellular solids: structure and properties,” 1999.

[2] A. du Plessis *et al.*, “Beautiful and Functional: A Review of Biomimetic Design in Additive Manufacturing,” *Addit Manuf*, vol. 27, 2019, doi: 10.1016/j.addma.2019.03.033.

[3] D. Bhate *et al.*, “Classification and Selection of Cellular Materials in Mechanical Design: Engineering and Biomimetic Approaches,” *Designs (Basel)*, vol. 3, no. 1, p. 19, Mar. 2019, doi: 10.3390/designs3010019.

[4] J. C. Maxwell, “On reciprocal figures and diagrams of forces,” *Philosophical Magazine*, vol. 4, no. 27, pp. 250–261, 1864.

[5] V. S. Deshpande, M. F. Ashby, and N. A. Fleck, “Foam topology: Bending versus stretching dominated architectures,” *Acta Mater*, vol. 49, no. 6, pp. 1035–1040, 2001, doi: 10.1016/S1359-6454(00)00379-7.
[6] A. H. Schoen, “Reflections concerning triply-periodic minimal surfaces,” *Interface Focus*, vol. 2, no. 5, pp. 658–668, 2012, doi: 10.1098/rsfs.2012.0023.
[7] J. W. Fisher, S. W. Miller, J. Bartolai, T. W. Simpson, and M. A. Yukish, “Catalog of triply periodic minimal surfaces, equation-based lattice structures, and their homogenized property data,” *Data Brief*, vol. 49, Aug. 2023, doi: 10.1016/j.dib.2023.109311.
[8] L. Han and S. Che, “An Overview of Materials with Triply Periodic Minimal Surfaces and Related Geometry: From Biological Structures to Self-Assembled Systems,” *Advanced Materials*, vol. 1705708, pp. 1–22, 2018, doi: 10.1002/adma.201705708.
[9] J. Wu, N. Aage, and O. Sigmund, “Infill Optimization for Additive Manufacturing – Approaching Bone-like Porous Structures,” *IEEE Trans Vis Comput Graph*, vol. 24, no. 2, pp. 1127–1140, 2017.
[10] O. Sigmund, “Design of Material Structures Using Topology Optimization.” Accessed: Feb. 05, 2019. [Online]. Available: https://www.researchgate.net/publication/261173987
[11] R. K. Luu *et al.*, “Learning from Nature to Achieve Material Sustainability: Generative AI for Rigorous Bio-inspired Materials Design,” *An MIT Exploration of Generative AI*, Mar. 2024, doi: 10.21428/e4baedd9.33bd7449.
[12] C. Ma *et al.*, “Accelerated design and characterization of non-uniform cellular materials via a machine-learning based framework,” 2020, doi: 10.1038/s41524-020-0309-6.
[13] G. X. Gu, C.-T. Chen, D. J. Richmond, and M. J. Buehler, “Bioinspired hierarchical composite design using machine learning: simulation, additive manufacturing, and experiment,” *Mater Horiz*, vol. 5, no. 5, pp. 939–945, Aug. 2018, doi: 10.1039/C8MH00653A.
[14] D. Novellino and Z. F. Ertug, “Baskets of the World: The Social Significance of Plaited Crafts,” in *Proceedings of the IVth International Congress of Ethnobotany (ICEB 2005)*, 2006. [Online]. Available: https://www.researchgate.net/publication/330261652
[15] sv Lomov, G. Perie, ds Ivanov, I. Verpoest, and D. Marsal, “Modeling three-dimensional fabrics and three-dimensional reinforced composites: Challenges and solutions,” *Textile Research Journal*, vol. 81, no. 1, pp. 28–41, 2011, doi: 10.1177/0040517510385169.
[16] K. Bilisik, N. S. Karaduman, N. E. Bilisik, and H. E. Bilisik, “Three-dimensional fully interlaced woven preforms for composites,” *Textile Research Journal*, vol. 83, no. 19, pp. 2060–2084, 2013, doi: 10.1177/0040517513487791.
[17] F. Boussu, I. Cristian, and S. Nauman, “General definition of 3D warp interlock fabric architecture,” *Compos B Eng*, vol. 81, pp. 171–188, 2015, doi: 10.1016/j.compositesb.2015.07.013.
[18] H. Agrawal, “InterWoven: Integrating Traditional Basket Weaving Craft into Computer Aided Design Signature redacted Signature redacted,” 2016.
[19] R. Wu *et al.*, “Weavecraft,” *ACM Trans Graph*, vol. 39, no. 6, Nov. 2020, doi: 10.1145/3414685.3417865.
[20] B. C. White, A. Garland, R. Alberdi, and B. L. Boyce, “Interpenetrating lattices with enhanced mechanical functionality,” *Addit Manuf*, vol. 38, no. September 2020, p. 101741, 2021, doi: 10.1016/j.addma.2020.101741.

[21] W. P. Moestopo, A. J. Mateos, R. M. Fuller, J. R. Greer, and C. M. Portela, “Pushing and Pulling on Ropes: Hierarchical Woven Materials,” *Advanced Science*, vol. 7, no. 20, pp. 1–8, 2020, doi: 10.1002/advs.202001271.
[22] Y. Mistry *et al.*, “Bio-inspired selective nodal decoupling for ultra-compliant interwoven lattices,” *Commun Mater*, vol. 4, no. 1, Dec. 2023, doi: 10.1038/s43246-023-00363-6.
[23] “Rhino 7,” 2023, *Robert McNeel & Associates, Seattle*.
[24] “Rhino 7,” 2023, *Robert McNeel & Associates, Seattle*. Accessed: Aug. 10, 2023. [Online]. Available: https://www.rhino3d.com/mcneel/about/
[25] EOS, “PA2200 Nylon Powder Material Properties.” Accessed: Jan. 05, 2019. [Online]. Available: https://www.3dhubs.com/material/eos-pa-2200
[26] “INSTRON North America.” [Online]. Available: www.instron.com
[27] D. Goss, Y. Mistry, B. Santhanam, C. Noe, S. Niverty, and C. Ozturk, “Bio-Inspired Honeycomb Core Design : An Experimental Study of the Role of Corner Radius , Coping and Interface,” *MDPI Biomimetics*, vol. under revi, pp. 1–16, 2020.
[28] Q. Lam *et al.*, “An examination of the low strain rate sensitivity of additively manufactured polymer, composite and metallic honeycomb structures,” *Materials*, vol. 12, no. 20, pp. 1–14, 2019, doi: 10.3390/ma12203455.
[29] ISO, *ISO 13314: Mechanical testing of metals, ductility testing, compression test for porous and cellular metals*. 2011. doi: ISO 13314:2011.
[30] M. Shinde, I. Ramirez-Chavez, D. Anderson, J. Fait, M. Jarrett, and D. Bhate, “Towards an Ideal Energy Absorber: Relating Failure Mechanisms and Energy Absorption Metrics in Additively Manufactured AlSi10Mg Cellular Structures under Quasistatic Compression,” *Journal of Manufacturing and Materials Processing*, vol. 6, no. 6, p. 140, 2022, doi: 10.3390/jmmp6060140.